E. GALENNE – S. ANDRIEUX – L. RATIER

A modal approach to linear fracture mechanics for dynamic loading at low frequency

RI-B3-N°002   Septembre 2006

A MODAL APPROACH TO LINEAR FRACTURE MECHANICS FOR DYNAMIC LOADING AT LOW FREQUENCY

E. GALENNE*,[#], S. ANDRIEUX*, L. RATIER[#]

*LaMSID, UMR CNRS EDF 2832,

[#]EDF R&D, Dept of Analysis in Mechanics and Acoustics

1 avenue du Général de Gaulle, 92141 Clamart Cedex, France

Abstract

In this paper, a modal approach to fracture mechanics for dynamic loading is proposed. This approach is based on the linear recombination of modal stress intensity factors. The modal stress intensity factors may be computed either from a classical crack-tip-opening-displacement method or by an energy method that is detailed in this paper. The energy method is based on a bilinear form stemming from the energy release rate quadratic form and it turns out to be very satisfactory -compared to other methods- in a large range of frequencies, up to moderate frequencies. The accuracy of the modal approach to fracture mechanics is discussed through several examples and demonstrated in an industrial application.

Keywords

Linear Fracture Mechanics, Modal Recombination, Energy Method.

1. INTRODUCTION

Fracture mechanics for dynamic loading is less commonly studied than static fracture mechanics unless industrial applications are varied: fatigue tests, rotating machines and seismic analysis. For low or moderate frequencies, the study of a fixed crack (non dynamically-propagating crack) may be conducted with the usual static criteria provided that both static and inertial effects are taken into account in the computation of fracture mechanics parameters.

Introduction of inertial effects in the energy release rate G is discussed by Destuynder [1,2] in order to define an active control of a cracked body for dynamic loads. For fast dynamical applications the Laplace transform is preferably used, as in [3] by Freund and Rice for infinite bodies and in [4] by Petroski for finite cracked beams: an elastodynamic weight function is defined from elastodynamic stress intensity factors corresponding to a reference dynamic load. This weight function is sufficient for accurately determining the time-dependent stress intensity factors corresponding to other dynamic loads of the same cracked structure.

Experimental identification of elastodynamic stress intensity factors is discussed by Bui et al. [5]. An engineering approach to cracked structures subjected to dynamic loading is proposed by Kuntiyawichai and Burderkin [6] and applied to seismic analysis. The J-integral including inertial effects is computed with a standard FEM method (Abaqus code). An approximate simplified method is used to get rid of the direct time integration method of the dynamic problem, which requires prohibitive computation time.

A modal approach is proposed by Doyle et al. [7], as the behavior of stress intensity factor K as a function of frequency is shown to be very similar to a modal response. Only static K calibration needs to be performed.

In a continuation of this last study, the aim of this paper is to propose a method for accurately and more efficiently solving fracture mechanics problems for structures with dynamic loading at low frequencies. This approach is based on the modal recombination, so that it is restricted to linear elasticity. Consequently, the contact between the crack faces is not taken into account. This assumption may appear as very restrictive, but it is met in most of industrial applications within the range of low frequency solicitations: the structure is often subjected to a preponderant static load that tends to open the crack. For instance, this is the case for cracked solids which are subjected to quasi-static inertial forces and which are oscillating around an equilibrium position. The aim of the mechanical analysis is either to determine if an existing crack will propagate, or to compute the rate of propagation of cracks for repeated dynamic loads.

For high frequency loads inertial effects locally change the crack singularity and affect the accuracy of the computation of stress intensity factors. Moreover, modal approaches are usually restricted to low or moderate frequencies. That is why for applications in fast dynamics -like impact response, direct computation should preferably be used.

In the first part of the paper, linear fracture mechanics equations are described and applied to harmonic problems. The modal recombination approach is derived and specialized to a cracked structure. This approach is based on the definition of *modal stress intensity factors*. Modal SIFs can be computed either by a classical crack-tip-opening-displacement method (CTOD) or by an energy method, which is detailed in the third part. This energy method is based on the computation of a bilinear form issued from the energy release rate quadratic

3

form. In the formula used, the singular solutions of elastodynamics are replaced by the static ones, and the quality of the approximation is evaluated. It turns out to be very satisfactory in a large range of frequencies, up to moderate frequencies.

In the last part, the modal approach is applied to a 2D and a 3D problem successively.

2. LINEAR FRACTURE MECHANICS FOR DYNAMIC LOADINGS

2.1. DEFINITIONS AND GENERAL EQUATIONS

Consider an elastic body Ω, containing a crack of length l, denoted by Γ_l. For the sake of simplicity, the presentation is restricted to two-dimensional problems. The displacement is prescribed to the value u_p on a part Γ_U of the boundary of the solid, initially at rest and stress-free and subjected to dynamic loading consisting of surface traction $\mathbf{R}$ on the remaining part Γ_R of its boundary and of body forces $\mathbf{f}$. Denoting by u the displacement field and by $\dot{u}$ its time derivative, the energies entering into the mechanical analysis of the solid are:

Elastic energy: $$W^{\text{el}}(u) = \frac{1}{2}\int_{\Omega} \mathbf{A} : \varepsilon(u) : \varepsilon(u) \tag{1}$$

Kinetic energy: $$W^{\text{kin}}(\dot{u}) = \frac{1}{2}\int_{\Omega} \rho \dot{u}^2 \tag{2}$$

Power of external forces: $$P(v) = \int_{\Omega} \mathbf{f}.v + \int_{\Gamma_R} \mathbf{R}.v \tag{3}$$

where $\mathbf{A}$ denotes the fourth order Hooke tensor, and ρ is the mass density.

The energy release rate G of the crack is classically defined as below [8,9]:

$$G = -\frac{d}{dl}\left(W^{\text{el}}(u) + W^{\text{kin}}(\dot{u}) - P(u)\right) \tag{4}$$

An alternative and completely equivalent formula is given in [10]:

4

$$G = -\frac{\partial}{\partial l}\left(W^{\text{el}}(u)\right) \tag{5}$$

The energy release rate is used in propagation criteria, but fracture mechanics problems are more commonly studied through the stress intensity factors (SIFs) K_I, K_{II} and K_{III} associated with the three opening modes of the crack. SIFs characterize the singularity of the stress field σ and of the displacement field u near the crack tip:

$$K_i(t) \propto \lim_{r \to 0}\left(\sigma_i(r,t)\sqrt{r}\right)$$

$$u(x,t) = u^R(x,t) + K_I(t)u_I^S(x) + K_{II}(t)u_{II}^S(x) + K_{III}(t)u_{III}^S(x) \tag{6}$$

where u_I^S, u_{II}^S and u_{III}^S are the singular asymptotic parts of the solution of the dynamic elastic problem and u^R is the regular part. The three SIFs depend on the geometry and on the loading, then on time t for dynamic situations.

The propagation of an existing crack is studied either by estimation of initiation criteria over a time period T:

$$\sup_{t \in [0,T]} G(t) \leq G^c \,, \; \sup_{t \in [0,T]} K_I(t) \leq K_I^c, \; \text{or} \; \sup_{t \in [0,T]} f(K_I(t), K_{II}(t), K_{III}(t)) \leq 0 \tag{7}$$

or, for fatigue crack propagation, by Paris' law, where n denotes the number of loading cycles and c and m are material properties:

$$\frac{dl}{dn} = c\Delta K_I^m \tag{8}$$

2.2. APPLICATION TO HARMONIC PROBLEMS

In this section, the harmonic problem is either a forced response to a prescribed load at the set pulsation ω or an eigenmode solution associated with this pulsation. In both cases, the

displacement field, the velocity field, and prescribed surface traction and displacement may be expressed as:

$$u(x,t) = U(x)\cos(\omega t + \varphi) \quad \dot{u}(x,t) = -\omega U(x)\sin(\omega t + \varphi)$$

$$\mathbf{R}(x,t) = r(x)\cos(\omega t + \varphi) \quad u_p(x,t) = U_p(x)\cos(\omega t + \varphi)$$

(9)

The definition (5) for G in harmonic dynamics gives:

$$G(u) = -\frac{\partial}{\partial l}\left(W^{\text{el}}(u)\right)$$

(10)

The general equation (4) with the harmonic displacement field gives another expression for G:

$$G(u) = -\frac{d}{dl}\left(\frac{1}{2}\int_{\Omega} \mathbf{A}:\varepsilon(U):\varepsilon(U)\cos^2(\omega t + \varphi) + \frac{1}{2}\int_{\Omega} \rho\omega^2 U^2 \sin^2(\omega t + \varphi) - \int_{\Gamma_R} r.U\cos^2(\omega t + \varphi)\right)$$

$$= -\frac{d}{dl}\left(\frac{1}{2}\int_{\Omega} \mathbf{A}:\varepsilon(U):\varepsilon(U) - \frac{1}{2}\int_{\Omega} \rho\omega^2 U^2 - \int_{\Gamma_R} r.U\right)\cos^2(\omega t + \varphi)$$

(11)

$$= -\frac{d}{dl}\left(W^{\text{el}}(U) - W^{\text{kin}}(U) - P(U)\right)\cos^2(\omega t + \varphi)$$

The equivalence between the two expressions may be proved by using the virtual power principle with $\dfrac{\partial U}{\partial l}$ as virtual field

$$\int_{\Omega(l)} \mathbf{A}:\varepsilon(U):\varepsilon(\frac{\partial U}{\partial l}) - \int_{\Omega(l)} \rho\,\omega^2 U.\frac{\partial U}{\partial l} = \int_{\Gamma_R} r.\frac{\partial U}{\partial l}$$

(12)

so that:

$$-\frac{\partial}{\partial U}\left(\frac{1}{2}\int_{\Omega} \mathbf{A}:\varepsilon(U):\varepsilon(U) - \frac{1}{2}\int_{\Omega} \rho\omega^2 U^2 - \int_{\Gamma_R} r.U\right).\frac{\partial U}{\partial l} = 0$$

(13)

Note that the two last terms in the bracket of (11) have a null partial derivative with respect to the crack length l. This feature results from the fact that derivatives of domain integrals with respect to the domain of integration for zero volume variation (as this is the case for variation of crack surface) do not vanish if and only if the integrand function behaves as r^{-1}

at the crack tip. Whereas this condition is satisfied for the elastic energy because of the $r^{-1/2}$ singularity of the strain tensor field, this is not the case for the kinetic energy (it behaves as r) and for the potential energy of volume forces as soon as the body forces are more regular than $r^{-3/2}$. Using this result and equation (13), identity between the total derivative of the mechanical energy with respect to the crack length and the partial derivative of the elastic energy with respect to the crack length is established.

The total derivative of energy quantities may be computed by efficient techniques stemming from domain variation theory (so-called theta methods) or from invariant theory (contour invariant integrals), therefore it is more suited for computation.

Lastly, and similarly to the well-known formula for the energy release rate in elastostatics, a formula may be derived thanks again to the virtual power principle:

$$G = \frac{1}{2}\left(\int_{\Gamma_R} r.\frac{\partial U}{\partial l} - \int_{\Gamma_U} \sigma(\frac{\partial U}{\partial l}).U.n \right) \cos^2(\omega t + \varphi) \tag{14}$$

For the case of a free vibration problem, U is an eigenmode associated with the eigenfrequency $2\pi/\omega$. With the preceding expression of G, the notion of modal energy release rate may be defined:

$$G_\omega(U) = -\frac{d}{dl}\left(\frac{1}{2}\int_\Omega \mathbf{A}:\varepsilon(U):\varepsilon(U) - \frac{1}{2}\int_\Omega \rho\omega^2 U^2 \right)\Big|_{\omega=\text{cste}} \tag{15}$$

$$\int_\Omega \rho U^2 = 1$$

Here the eigenfrequency $2\pi/\omega$ is naturally a function of the crack length. However, attention must be paid to keep ω constant during the total derivation involved in the definition of the modal energy release rate. This perhaps paradoxical feature may be explained by using the Rayleigh quotient property:

$$\int_\Omega \mathbf{A}:\varepsilon(U):\varepsilon(U) - \int_\Omega \rho\omega^2 U^2 = 0 \quad \text{or} \quad \omega^2 = \frac{\int_\Omega \mathbf{A}:\varepsilon(U):\varepsilon(U)}{\int_\Omega \rho U^2} \tag{16}$$

so that we obtain the following result:

$$\frac{d}{dl}\left(\frac{1}{2}\int_{\Omega}\mathbf{A}:\varepsilon(U):\varepsilon(U)-\frac{1}{2}\int_{\Omega}\rho\omega^{2}U^{2}\right)=0 \tag{17}$$

which shows that a trivial result is obtained if ω is not kept constant during the total derivation in eq. (15). It also leads to an interesting characterization of the modal energy release rate:

$$G_{\omega}(U)=-\frac{1}{2}\frac{d\omega^{2}}{dl} \tag{18}$$

2.3. ANALYTICAL ILLUSTRATION

The purpose of this section is to apply and to compare the two different expressions of modal energy release rate for a simple case for which the energy is analytically known. Consider a structure composed of two springs, one of them being of variable stiffness $k(\alpha)$, see Figure 1. Here α plays the role of a "damage parameter". This model may be seen as the representation of a cracked specimen (rigidity equal to $k(\alpha)$) subjected to a load through a machine test, whose rigidity is k_0.
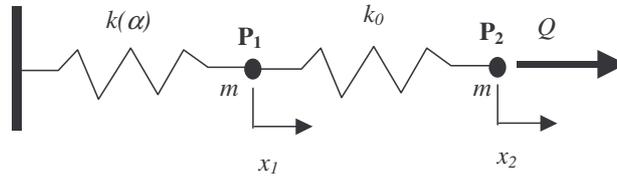

Figure 1 : The two-springs structure.

The structure is subjected to a prescribed harmonic force or to a prescribed harmonic displacement at point P_2. Equal masses m are placed at P_1 and P_2. The displacement field is written as $x_i(t)=X_i\cos(\omega t)$, $i=1,2$.

Equation (10) applied to the two-spring structure gives the simple expression of energy release:

$$G = -\frac{\partial}{\partial \alpha}\left(\frac{1}{2}k(\alpha)x_1^2 + \frac{1}{2}k_0(x_1 - x_2)^2\right) = -\frac{1}{2}k'(\alpha)x_1^2 \tag{19}$$

The dynamic equilibrium equations for lumped masses P_1 and P_2 are:

$$\begin{cases} (k_0 + k(\alpha) - m\omega^2)X_1 - k_0 X_2 &= 0 \\ (k_0 - m\omega^2)X_2 - k_0 X_1 &= Q \end{cases} \tag{20}$$

For harmonic displacement $X\cos(\omega t)$ prescribed at P_2, the solutions for the displacements are then:

$$X_2 = X \quad, \quad X_1 = \frac{k_0}{k(\alpha) + k_0 - m\omega^2}X \tag{21}$$

So that the energy release rate (10) is:

$$G^X = -\frac{1}{2}\frac{k'(\alpha)k_0^2}{\left(k(\alpha) + k_0 - m\omega^2\right)^2}X^2\cos^2\omega t \tag{22}$$

For a harmonic force $Q\cos(\omega t)$ prescribed at P_2, the solutions for the displacements and the modal energy release rate are:

$$X_1 = \frac{k_0}{\Delta(\omega)}Q, \qquad X_2 = \frac{k_0 + k(\alpha) - m\omega^2}{\Delta(\omega)}Q \tag{23}$$

$$G^Q = -\frac{1}{2}\frac{k'(\alpha)k_0^2}{\Delta^2(\omega)}Q^2\cos^2\omega t \tag{24}$$

with $\Delta(\omega) = k_0 k(\alpha) - m\omega^2\left(2k_0 + k(\alpha)\right) + m^2\omega^4$.

It is noticeable that G^Q and G^X are equal when Q and X are related via the solution of the elastic dynamic equilibrium equations (20) as this is the case in elastostatics. It may also be easily verified that the results are the same with the alternative equation (11). Indeed, for the case of prescribed displacement X:

$$G = -\frac{d}{d\alpha}\left(\frac{1}{2}k(\alpha)x_1^2 + \frac{1}{2}k_0(x_1 - x_2)^2 - \frac{1}{2}m\omega^2(x_1^2 + x_2^2)\right)$$

$$= -\frac{d}{d\alpha}\left(\frac{1}{2}Qx_2\right) = -\frac{1}{2}\frac{d}{d\alpha}\left((k_0 - m\omega^2) - \frac{k_0^2}{k_0 + k(\alpha) - m\omega^2}\right)X^2\cos^2\omega t \tag{25}$$

which is the result of equation (22).

For the case of the prescribed force Q, equation (4) is:

$$G = -\frac{d}{d\alpha}\left(\frac{1}{2}k(\alpha)x_1^2 + \frac{1}{2}k_0(x_1 - x_2)^2 - \frac{1}{2}m\omega^2(x_1^2 + x_2^2) - Qx_2\right)$$

$$= -\frac{d}{d\alpha}\left(-\frac{1}{2}Qx_2\right) = \frac{1}{2}Q^2\left[\frac{k'(\alpha)}{\Delta} - \frac{(k_0 + k(\alpha) - m\omega^2)}{\Delta^2}(k_0 - m\omega^2)k'(\alpha)\right]\cos^2\omega t \tag{26}$$

$$= -\frac{1}{2}\frac{k_0 k'(\alpha)}{\Delta^2}Q^2\cos^2\omega t$$

which again is the result of equation (24).

3. MODAL DECOMPOSITION FOR THE DYNAMIC RESPONSE OF A CRACKED SOLID

3.1. MODAL RECOMBINATION AND CRACK SINGULARITY

The displacement $u(x,t)$ solution of a dynamic linear problem may be approximated by its decomposition on a truncated basis of eigenmodes $\Phi^i(x)$ according to the Ritz Method [11]:

$$u(x,t) = \sum_{i=1}^{M}\alpha_i(t).\Phi^i(x) \tag{27}$$

The accuracy of the modal recombination depends on the number M of eigenmodes in the basis, and convergence results exist for the displacement field and the strain field [12].

At the tips of the crack, the jump of the displacement field may be described by the three SIFs. If $(\mathbf{N},\mathbf{T},\mathbf{V})$ is a local direct Cartesian frame located at a point M of the crack tip with

the normal (**N**) to the tangent plane to the crack and the tangent vector (**T**) to the crack tip curve, the following asymptotic relations hold:

$$K_I(s,t) = \lim_{r \to 0} \left(\frac{E}{8(1-v^2)} [\![u_N(r,s,t)]\!] \sqrt{\frac{2\pi}{r}} \right)$$

$$K_{II}(s,t) = \lim_{r \to 0} \left(\frac{E}{8(1-v^2)} [\![u_T(r,s,t)]\!] \sqrt{\frac{2\pi}{r}} \right) \qquad (28)$$

$$K_{III}(s,t) = \lim_{r \to 0} \left(\frac{E}{8(1+v)} [\![u_V(r,s,t)]\!] \sqrt{\frac{2\pi}{r}} \right)$$

where r is the distance to the crack tip point, in the (**N,T**) plane, s is the curvilinear abscissa along the crack front and $[\![.]\!]$ denotes the jump operator across the crack along the local normal (**V**) to the crack front, directed towards the interior of the solid.

Combining equations (26) and (27) gives a new expression of the SIFs (in the sequel expression, it is given for mode I):

$$K_I(s,t) = \sum_{i=1}^{M} \alpha_i(t) . K_I^i(s) \qquad (29)$$

where $K_I^i(s)$ is the *modal stress intensity factor* of the ith eigenmode:

$$K_I^i(s) = \lim_{r \to 0} \left(\frac{E}{8(1-v^2)} [\![\Phi^i(r,s)]\!] \sqrt{\frac{2\pi}{r}} \right) \qquad (30)$$

For in-plane propagation, the modal energy release rate G_{ω_i} defined in equation (14) and the modal SIFs are related by Irwin's formula, which is the same in dynamic problems as in static problems [10]:

$$G_{\omega_i} = \frac{1-v^2}{E} \left((K_I^i)^2 + (K_{II}^i)^2 \right) + \frac{1}{\mu} (K_{III}^i)^2 \qquad (31)$$

11

where E is Young's modulus, ν Poisson's ratio and μ the second Lamé coefficient. For crack growth under mixed mode conditions and bifurcation, eq. (30) is no longer used and propagation criteria are written as a function of the three SIFs like in eq. (7).

The modal stress intensity factors are time-independent quantities: for 3D problems, they depend on the curvilinear abscissa; for 2D problems, they are scalars.

The crucial point here is that the coefficients $\alpha_i(t)$ of the combination (29) are the same as the coefficients of equation (27) for the displacement field. These coefficients are computed in most of the standard finite element codes dealing with low frequency dynamical applications.

Once the linear dynamical response of the structure for the prescribed load has been computed on the subspace generated by the number M of eigenmodes (i.e. identification of $[\alpha_i(t)]$), solving the fracture mechanics problem may then be achieved in two steps:

- identification of the M first modal SIFs (a computation that is independent of the loads prescribed to the structure; and may be done once and for all);

- recombination through equation (29) to obtain the time-dependent SIFs.

This approach is clearly more computationally efficient than the classical one. Indeed the classical approach consists of computing at each time step the estimation of the SIFs via equation (28). With the modal approach, the maximum values of linear fracture mechanics parameters such as K_I or the energy release rate G, may then be assessed with the highest precision.

3.2. COMPUTATION OF MODAL STRESS INTENSITY FACTORS

The asymptotic relation (29) provides a technique to extract the modal SIFs from a known (computed) eigenmode via the Crack Tip Opening Displacement method. In the sequel, a

refined version of the CTOD method by a least square identification procedure based on the displacement jump across the crack tip is used. More specifically, given a small length r_m, an approximation of the SIF K_I is computed as the solution of the least-squares minimization problem:

$$\tilde{K}_I^i(s) = \arg\min_k \int_0^{r_m} \left(\frac{E\sqrt{2\pi}}{8(1-v^2)} \left[\left[\Phi^i(r,s) \right]\right] - k\sqrt{r} \right)^2 dr \qquad (32)$$

This problem has a closed form solution which is a linear function of the displacement field for a given length r_m:

$$\tilde{K}_I^i(s) = \frac{E\sqrt{2\pi}}{4(1-v^2)r_m^2} \int_0^{r_m} \left[\left[\Phi^i(r,s) \right]\right] \sqrt{r} dr \qquad (33)$$

The CTOD method is well known for its simplicity and its ease of implementation in a FEM software package. Its accuracy is satisfactory and may be improved by the use of quarter-point elements at the crack tip [13]. In the following section, computation of modal SIFs based on an energy approach, which is less sensitive to the quality of the mesh and to the value of parameter r_m, is presented.

4. A STABLE ENERGY METHOD FOR THE COMPUTATION OF MODAL STRESS INTENSITY FACTORS

4.1. BILINEAR FORM OF THE STATIC ENERGY RELEASE RATE

For static problems, a bilinear form can be defined from the classical quadratic form of the energy release rate G, with the following properties:

$$\begin{cases} g(u,v) \in \mathcal{L}(H^1(\Omega) \times H^1(\Omega)) \\ g(u,v) = \dfrac{1}{4}\left(G(u+v) - G(u-v) \right) \end{cases} \qquad (34)$$

The bilinear form of G is very useful as it separates the three opening modes of the crack:

13

$$g(u, u_I^S) = \frac{1-v^2}{E} K_I(u), \quad g(u, u_{II}^S) = \frac{1-v^2}{E} K_{II}(u), \quad g(u, u_{III}^S) = \frac{1}{2\mu} K_{III}(u) \qquad (35)$$

where u_I^S, u_{II}^S and u_{III}^S are the singular solutions corresponding to the three opening modes of the crack.

$$\begin{cases} u_I^S = \dfrac{1+v}{E} \sqrt{\dfrac{r}{2\pi}} (k - \sin\theta) \left(\cos\left(\dfrac{\theta}{2}\right) \vec{e}_V + \sin\left(\dfrac{\theta}{2}\right) \vec{e}_N \right) \\[2ex] u_{II}^S = \dfrac{1+v}{E} \sqrt{\dfrac{r}{2\pi}} (k + \cos\theta + 2) \left(\sin\left(\dfrac{\theta}{2}\right) \vec{e}_V + \cos\left(\dfrac{\theta}{2}\right) \vec{e}_N \right) \\[2ex] u_{III}^S = \dfrac{4(1+v)}{E} \sin\left(\dfrac{\theta}{2}\right) \sqrt{\dfrac{r}{2\pi}} \vec{e}_T \end{cases} \qquad (36)$$

in the local Cartesian frame (**N**,**T**,**V**) as defined in 3.1, with $k = 3 - 4v$. The singular displacements are analytically calculated for 2D problems only (plane and antiplane), but it is shown in [9] that the displacement field near the crack front in 3D may be obtained by the sum of the three classical singular displacements and of four other particular displacements, which nevertheless are more regular. If the crack front is sufficiently regular, the displacement field has the same asymptotical behavior.

The properties of g stated in equation (35) is a consequence of the orthogonality of singular displacements for the bilinear application $g(u,v)$ and is demonstrated by using the Rice J-integral (with $J = G$ in linear elastic fracture mechanics), with considerations of symmetry of singular displacements and with the Irwin formula. This approach, developed by Bui [14], provides a new computation method for SIFs and is quite commonly used [15].

From a numerical point of view, the energy release rate G and, then, its associated bilinear form g may be calculated by a θ-method [16,17,18]. The method is based on a virtual displacement field θ and all derivatives with respect to the crack growth can be computed by using a Lagrangian method. For 3D problems, local values $G(s)$ and $K(s)$ are computed by introducing local θ fields. θ fields are geometrically defined from two rings around the crack front (radius R_{inf} and R_{sup}) but G is theoretically independent of this rings. The

14

geometrical definition of the θ field around the crack tip and the variation of $|\theta|$ as a function of the distance to the crack tip are given in Figure 2.
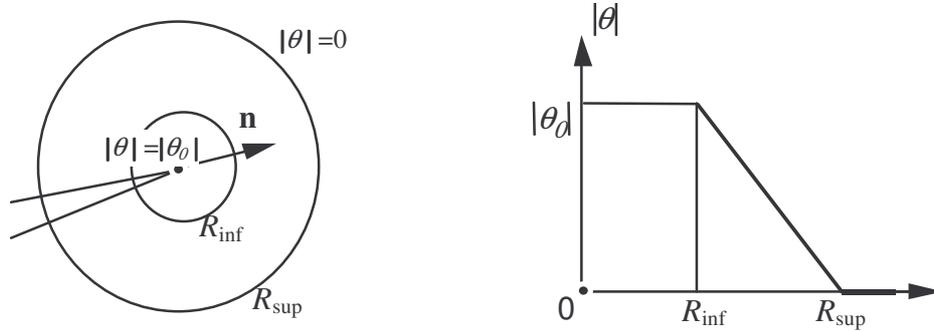

Figure 2. Geometrical definition of the θ field around the crack tip and variation of $|\theta|$ as a function of the distance to the crack tip.

Comparisons with other computation methods [19] show that the θ-method is very accurate and to a large extent, mesh-independent.

4.2. EXTENSION TO HARMONIC PROBLEMS

The properties (35) of the bilinear form associated with the static energy release rate G may be extended without any difficulty to harmonic problems. However, the singular harmonic displacements u_I^S, u_{II}^S and u_{III}^S for a given circular frequency are up to now not available. Antiplane problems are the only case where the singular harmonic field, reduced to a scalar, can be expressed and it is found to be proportional to $\sin(\omega r)/\omega r$: although this is clearly dependent on the circular frequency, it is easy to ascertain that the asymptotic behavior is exactly the static antiplane singular solution field [10].

For other situations, it is however possible to assume that the singular harmonic displacements have the same asymptotic form as in elastostatics, so that an estimation of the modal SIFs may be obtained by using the static singular displacement fields. The results will however no longer be independent of the geometrical definition of the integration area

15

and of the frequency. The error introduced by the static singular displacements in the computation of jth modal SIF may be estimated with:

$$E_j(\theta) = \left| \frac{\sqrt{G_\theta^{\text{Irwin}}(\varphi_j, u_I^S, u_{II}^S, u_{III}^S)} - \sqrt{G_\theta(\varphi_j)}}{\sqrt{G_\theta(\varphi_j)}} \right| \tag{37}$$

where G_θ^{Irwin} is the energy release rate identified with the Irwin formula (31) from the modal SIF obtained by the θ-method and equation (35). The exact value G_θ is directly computed from the eigenmode Φ^j by the θ-method and is independent of the integration area.

In Figure 3, the error $E_j(\theta)$ is depicted (for the 2D example described in the following section) for three different integration areas characterized by the radius R_{sup} of their outer θ-ring. The radius R_{inf} of their inner θ-ring is constant. The error increases with the order of the eigenmode, thus with the eigenfrequency, but it is noticeably less important for the two smaller integration areas.
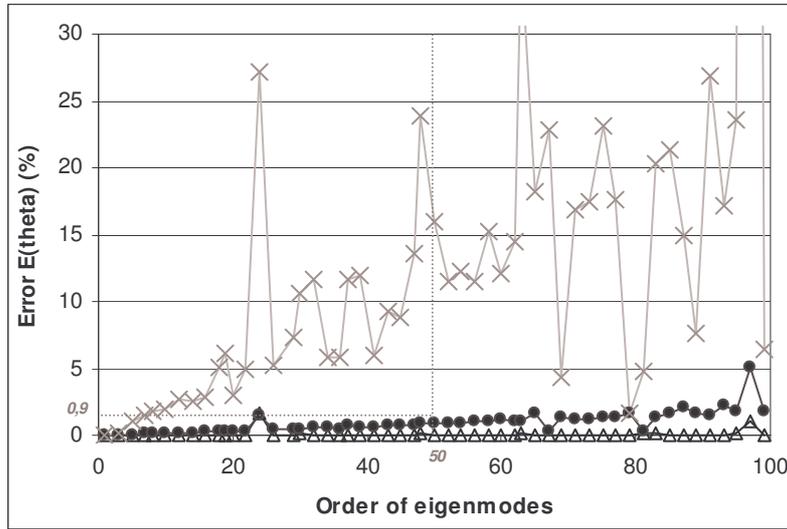

Figure 3. Influence of the geometrical integration area (outer radius R_{sup}) on modal SIFs identification accuracy:
$\times$, $R_{\text{sup}} = l/50$; $\bullet$, $R_{\text{sup}} = l/5$; $\triangle$, $R_{\text{sup}} = l/1.25$ where l is the crack length.

16

Note that the evolution of $E_j(\theta)$ is not monotonic with j. This is a consequence of the modal effect on the crack, which is very different from one mode to the other.

The error in the 50th mode is less than 1% for an outer integration ring corresponding to one fifth of the crack length. The energy method proposed here is accurate for moderate frequencies if the integration area remains in the vicinity of the crack front. The integration area must be smaller as the frequency increases.

5. APPLICATIONS

The presented modal approach will be successively applied to a 2D simple model and to a 3D example and will be illustrated with an industrial application. All numerical computations were performed with the *Code_Aster* [20], which is the numerical simulation software package for structural analysis developed by EDF R&D.

5.1. 2D SIMPLE TEST

In this section, the structure is a slender two-dimensional beam (plane stress model). The dimensions of the beam are chosen so as to approach the industrial case of the final blade of a turbine of nuclear power stations. A small crack (15% of total width) is positioned at the 2/5 of the height of the beam, see Figure 4.

The mesh of the beam has 2,000 nodes and 700 quadratic elements and is refined around the crack tip. The first frequency f_1 of this structure lies at 340 Hz. A slight damping coefficient is introduced in material properties. The nodes of the lower segment of the beam are fixed; the mechanical load is a prescribed force F_x on the nodes of the higher segment in horizontal direction.
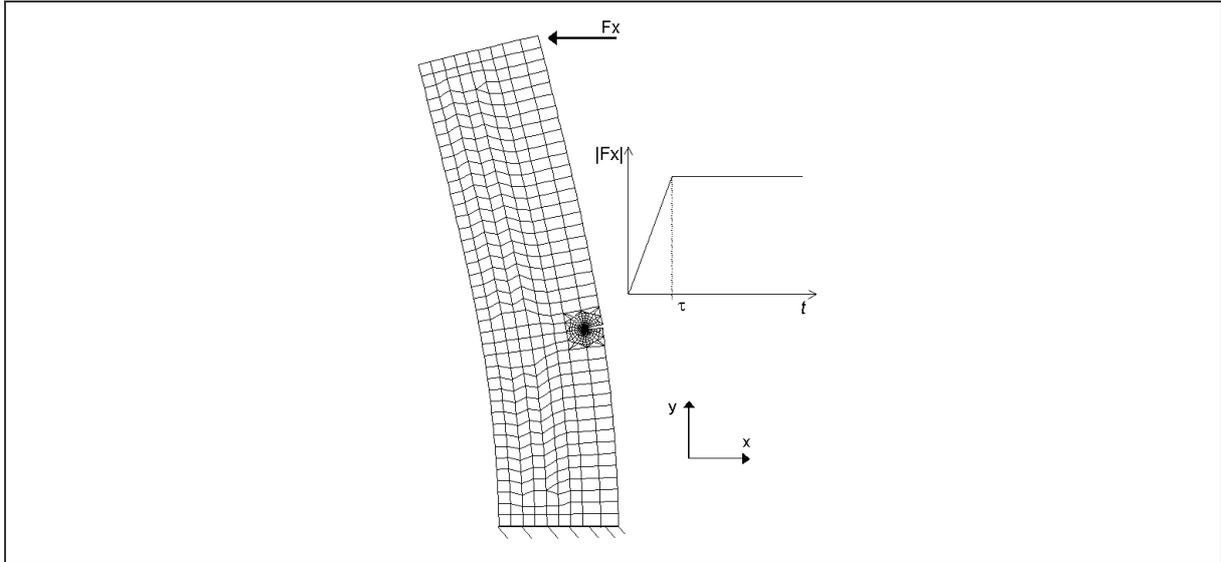
Figure 4. Deformed mesh of the cracked 2D beam at time τ
and definition of the ramp bending load.

The amplitude of the force is time-dependent:

$$F_x = 0 \text{ for } t<0;$$

$$F_x = 1 \text{ for } t>\tau;$$

$$F_x \text{ is linear for } t \text{ in }]0, \tau[.$$

τ characterizes the slope of the ramp load. A static vertical force is also imposed on the upper part of the beam so as to have an open crack at all times. The mechanical problem is then linear. Only the opening mode of crack, characterized by the value of K_I, is considered. K_{II} is much lower than K_I.

The variation of K_I as a function of time is depicted in Figure 5. During the loading phase K_I is increasing; when F_x is constant K_I is oscillating at the beam's first frequency. The amplitude of the vibration is increasing with the ramp rate τ: the maximum of $K_I(t)$ is $1.1K_I^{\text{stat}}$ for $\tau=3/f_1$ and $1.85K_I^{\text{stat}}$ for $\tau=0.3/f_1$, where K_I^{stat} is the static value of K_I for $F_x=1$. It is noticeable that the time course of K_I is relevant to the usual time course of displacements for such ramp loads since the SIFs are linear functions of the displacement field (33).
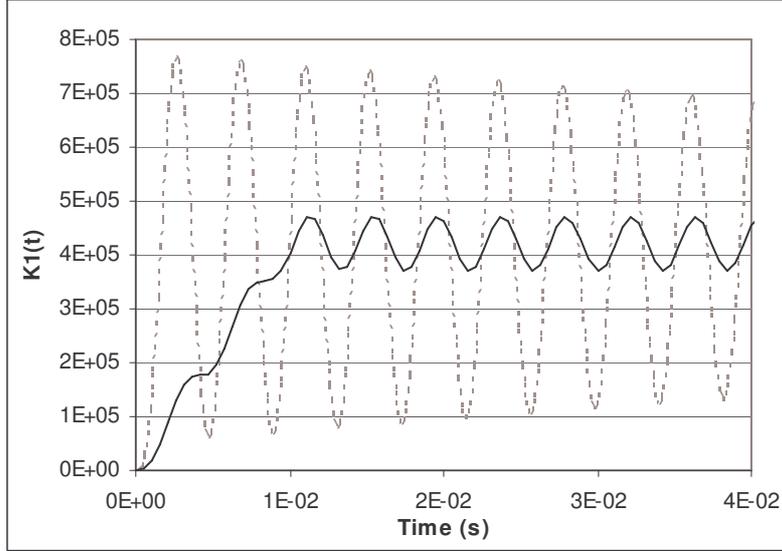
18

Figure 5. Influence of ramp rate τ on the variation of $K_I(t)$ (MPa.$\sqrt{}$m): $\tau = 3/f_1$ (solid line) and $\tau = 0.3/f_1$ (dotted line).

The difference between the modal SIFs identified by the CTOD method and by the energy method is between 0.5 and 5%, but the energy method is noticeably less dependent on the integration area geometrical parameters: a multiplication by two of the number of elements in the integration area leads to a mean K_I variation of 0.6 % in the energy method and of 4.6% in the CTOD method.

The precision of the modal approach is studied by comparison with results of a full explicit computation of the transient problem (Newmark explicit integration scheme). Denoting by q_n, a time-dependent quantity calculated by modal recombination from n modes and by $q_{\exp}$, the same quantity computed by an explicit method, the error in q is defined as:

$$E_q(n) = 1 - \frac{\sup_t q_n(t)}{\sup_t q_{\exp}(t)} \qquad (38)$$

The convergence of the computation with the number of modes of the recombination is depicted in Figure 6 for $\tau = 3f_1$. Convergence rates of the SIFs computed with the two methods are very close and comparable with the convergence rate of the displacements (here the horizontal displacement u_x extracted in the middle of the highest segment of the

19

beam). With 30 recombination modes, the error in the three quantities is around 0.1 % and accumulated mass is about 97 % of total mass.
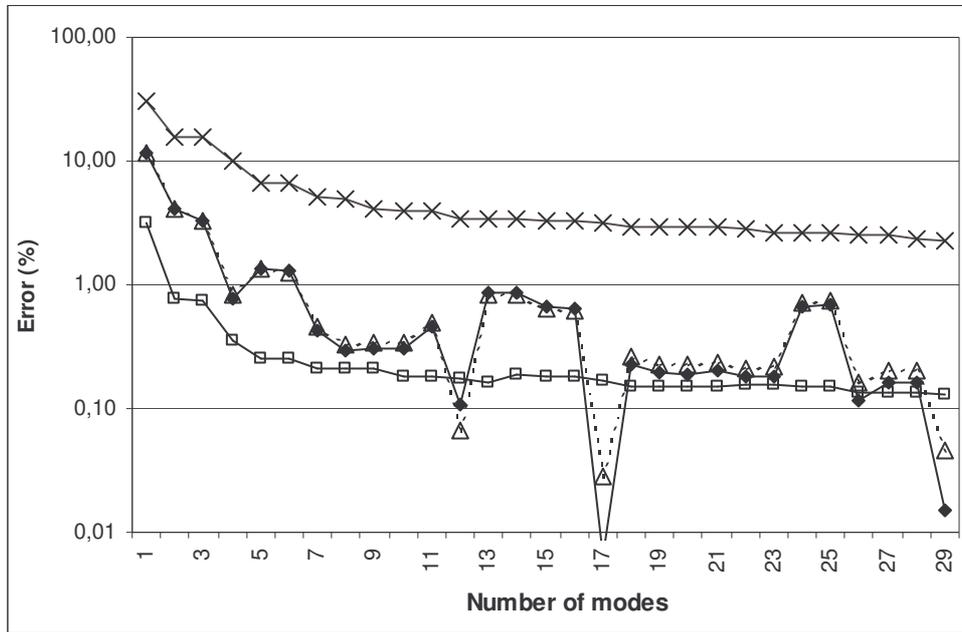

Figure 6. Convergence on K_I -computed with θ-Method (◆) or CTOD Method (△)-, horizontal displacement (□) and accumulated mass (×) with the number of recombination modes.

The convergence rates of SIFs are however very irregular, which can be explained by a study of modal quantities: modal SIFs are very heterogeneous (K_I^{12} / K_I^{11} = 50) whereas all modal displacements have the same order of magnitude (u_x^{12} / u_x^{11} = 0.5). General results do not exist to determine the number of required modes for each problem. However some criteria, as for instance accumulated mass, are used in practice by engineers; these criteria can also be used for fracture mechanics, as the convergence rate of the SIFs is coherent with the convergence rates of displacements and of the accumulated modal mass.

The computation of a dynamic problem by means of a modal approach is very less time-consuming than full explicit computation. Identification and recombination of modal SIFs is also faster than identifying the SIFs from explicit displacement field at each time step. The modal approach to fracture mechanics takes approximately 40 times less computation time than the explicit scheme.

5.2. 3D EXAMPLE

The 3D structure is generated by extrusion of the previous 2D mesh with 10 elements in its depth, see Figure 7. The cracked beam, whose thickness is a tenth of its width, is subjected to a ramp bending load. The load rate τ is equal to $0.3\, f_x^1$ where f_x^1 is the frequency of the first flexion mode in direction **x**, see Figure 4. The load is defined in such a way that the three opening modes of the crack are activated ($F_z(t) = 0.4 F_x(t);\ F_y = $ constant).
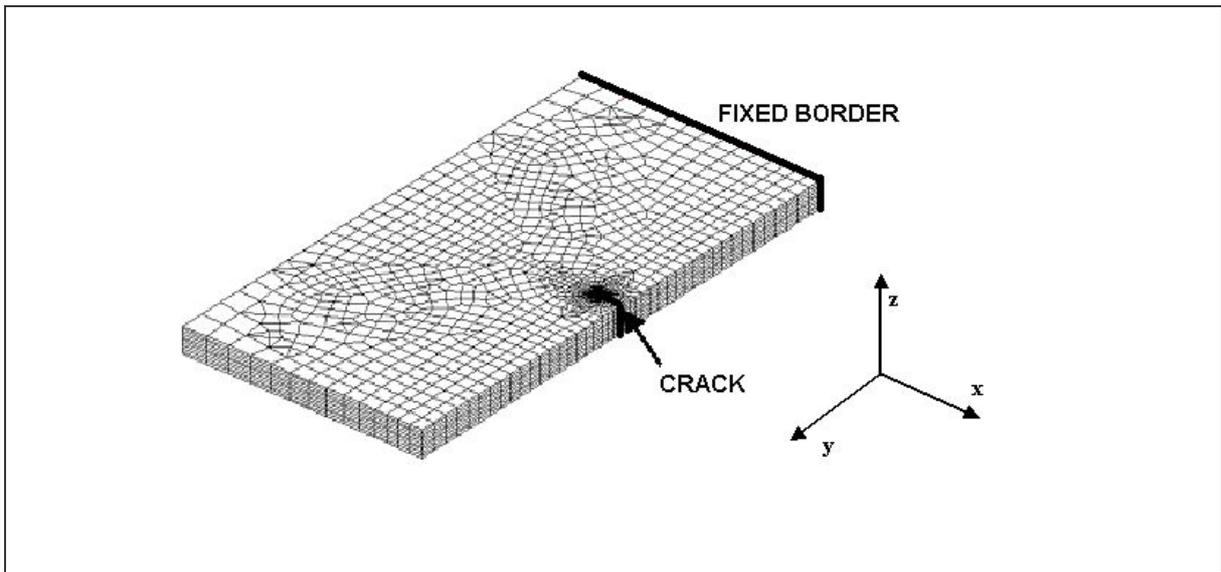

Figure 7. Mesh of the cracked 3D beam.

The variation of the three SIFs versus time is depicted in Figure 8. The vibration of the beam on the first flexion mode in direction **x** leads to slight oscillations of $K_I(t)$; vibrations on the first flexion mode in direction **z** lead to slower and pronounced oscillations of $K_I(t)$ and $K_{III}(t)$. K_{II} and K_{III} are less important than K_I but not negligible.

The first two flexion modes are noticeably predominant on the cracked structure behavior. The results of the modal approach are successfully compared to the results of an explicit scheme (Newmark explicit integration scheme).
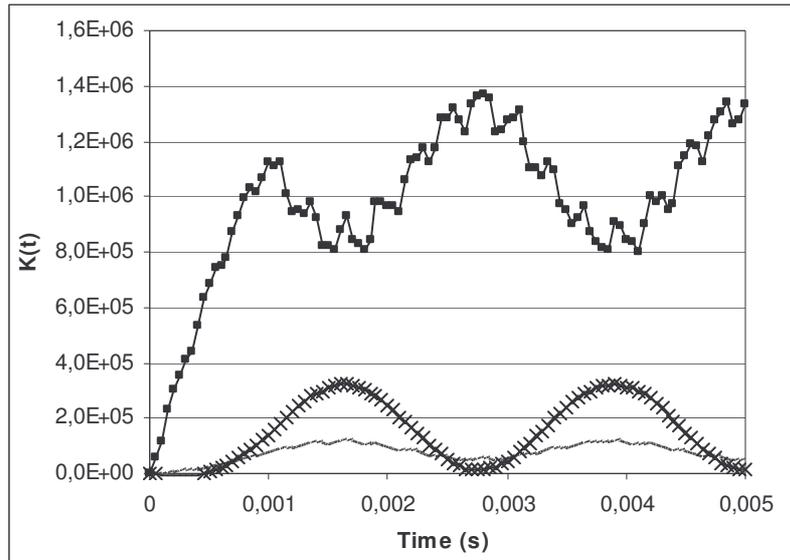
Figure 8. Evolution of SIFs (MPa.√m) at the middle node of the crack front:
■, $K_I(t)$; ×, $K_{II}(t)$; --, $K_{III}(t)$.

The number of modes in the recombination basis must nevertheless be larger for this 3D computation than in the previous 2D-example: with 60 recombination modes the error in K_I is less than 2 %, the error in vertical displacement is 0.3 % and accumulated mass is around 95 % of total mass. The computation times of the modal approach are again much lower than those of the explicit scheme.

5.3. INDUSTRIAL APPLICATION

In this section, the strategy exposed earlier is used for an industrial application. Let us consider a large blade of a low-pressure steam turbine. The blade is 1.5 meters long and it is located at about 1.2 meters from the axis of rotation. Hence, the blade is exposed to very high mechanical stresses due to centrifugal effects at high rotational speed (1,500 rpm) and to dynamic stresses induced by flow pressure fluctuations. A crack is located in the upper hook of the root of the fir-tree blade and its depth is equal to 40 % of total blade length, see Figure 9a. The purpose of this simulation is to determine whether the crack might

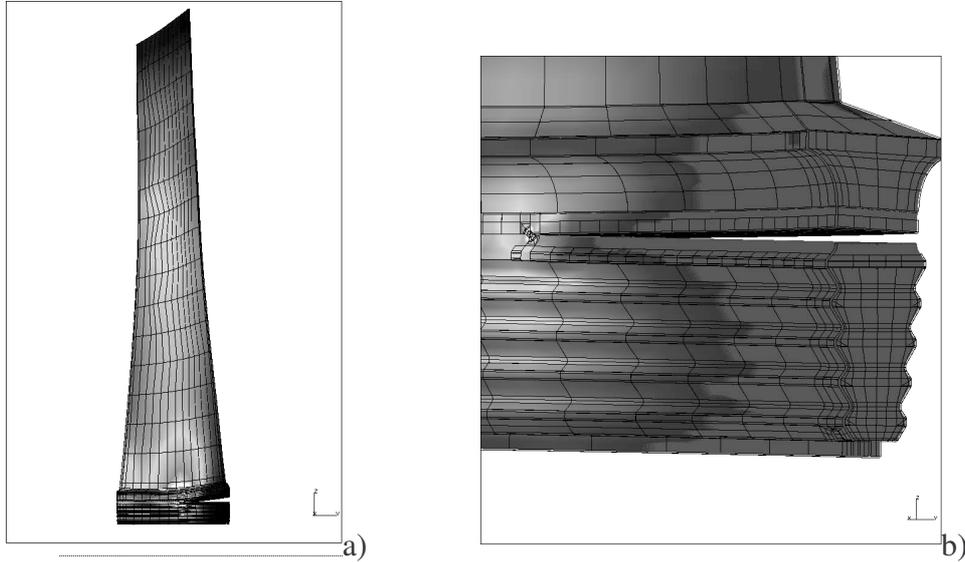propagate or not due to both centrifugal and dynamic stresses. The finite element mesh includes 40,000 nodes.

Figure 9. Deformation of the cracked fir-tree attachment blade subjected to a centrifugal load (a) and Von Mises' stress near the crack front (b).

Centrifugal load: The centrifugal load tends to open the crack. The maximum opening of the lips is 1.8mm. Von Mises' stress field on the deformed blade is depicted in Figure 9. The classical CTOD method gives a stress intensity factor value for each node of the crack front. The crack response is mainly on its first mode. Consequently, only the first opening mode is taken into account in the following.

These stress intensity factors are compared to the crack propagation threshold (10MPa.√m). It confirms that the crack is growing for each start and stop of the turbine. However, by using Paris' principle (8), it could be noticed that this growth is very small. Insofar that the number of start and stop cycles is less than one hundred, this propagation remains negligible.

Dynamical load: The dynamic load is unknown and difficult to compute. Preferably, a tip timing measurement method is used to identify the vibration amplitudes: the peaks of a Fast Fourier Transform (FFT) frequency spectrum give the modal contributions. The first three

vibration modes are predominant and their maximum modal amplitudes are: $\alpha_1^{\text{max}} = 1.51$, $\alpha_2^{\text{max}} = 0.0021$ and $\alpha_3^{\text{max}} = 0.184$, respectively.
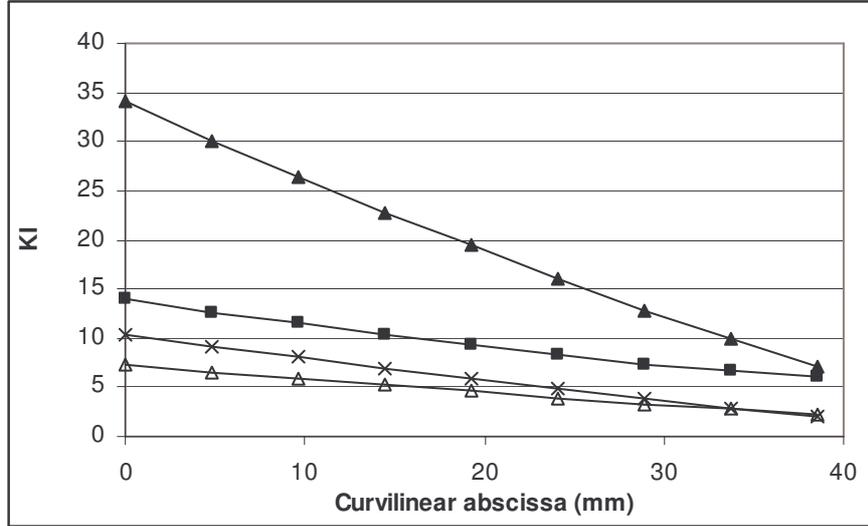

Figure 10. Stress intensity factor K_I (in MPa.$\sqrt{m}$) along the crack:
modal SIFs for first ($\times$), second ($\blacksquare$) and third mode ($\triangle$) of the structure
and amplitude of K_I due to the dynamic load ($\blacktriangle$).

The modal approach to fracture mechanics is used to compute the maximum of SIF $K_I^{\text{dyn}-\text{max}}$ due to the dynamic load:

$$K_I^{\text{dyn}-\text{max}}(s) = \max_t \left(\sum_{i=1}^{\infty} \alpha_i(t) K_I^i(s) \right) \approx \max_t \left(\sum_{i=1}^{3} \alpha_i(t) K_I^i(s) \right) \leq \sum_{i=1}^{3} \alpha_i^{\text{max}} K_I^i(s) \qquad (39)$$

The amplitude of K_I due to the dynamic load is depicted in Figure 10 and is equal to $2K_I^{\text{dyn}-\text{max}}$ as the static SIF is much greater than the dynamic one. The amplitude of K_I is higher than the crack propagation threshold and corresponds to fast propagation at each vibration of the structure and, will consequently lead to the failure of the blade. This kind of large crack is unacceptable for in-service conditions, when the dynamic load is as severe as measured in this turbine.

6. CONCLUSION

The energy method prescribed to compute the modal stress intensity factors proves to be satisfactory in a large domain of frequencies. This method based on the energy release rate quadratic form is less dependent on the mesh and on the integration area than the classical crack-tip-opening-displacement method.

The convergence rate of the modal recombination of SIFs is on average the same as the convergence rate of the modal recombination of the displacement field. The modal approach is also significantly less time-consuming than an explicit computation method: in the 2D and 3D-examples, the modal recombination takes 10 to 40 times less time than Newmark's explicit computation.

The modal approach to fracture mechanics is then an efficient and accurate method for studying the fatigue propagation of cracks in structures under dynamic load conditions. Once the linear dynamical response of the structure for the prescribed load has been computed on the subspace generated by a number M of eigenmodes, only two steps are required:

- identifying the M first modal SIFs with the energy method (a computation that is independent of the loads prescribed to the structure and may be done once and for all);

- modal recombination to obtain the time dependent SIFs.

With the modal approach, dynamic studies on 3D-structures may then be carried out, which were up to now very difficult or even impossible. The maximum values of linear fracture mechanics parameters are easy to compute with the highest precision and even, as a consequence of equation (18), the change in the eigenfrequencies of a structure with the propagation of the crack from the modal energy release rate may be predicted.

REFERENCES

1. P. Destuynder, Une approche du contrôle de la propagation des fissures en dynamique des structures, *Compte-Rendu de l'Académie des Sciences 306* (II) (1988), 953-956.

2. P. Destuynder, Computation of an active control in fracture mechanics using finite elements, *European Journal of Mechanics 9* (2) (1990), 133-141.

3. L.B. Freund, J.C. Rice, On the determination of elastodynamic crack tip stress fields, *International Journal of Solids and Structures 10* (1974), 411-417.

4. H.J. Petroski, J.L. Glazik, J.D. Achenbach, Construction of a dynamic weight function form a finite element solution of a cracked beam, *J. Applied Mechanics 47* (1980), 51-56.

5. H. D. Bui, H. Maigre, D. Rittel, A new approach to the experimental determination of the dynamic stress intensity factor, *International Journal of Solids and Structures* 29 (1992), 2881-2895.

6. K. Kuntiyawichai, F.M. Burderkin, Engineering assessment of cracked structures subjected to dynamic loads using fracture mechanics assessment, *Engineering Fracture Mechanics 70* (2003), 1991-2014.

7. J.F. Doyle, S.A. Rizzi, Frequency domain stress intensity calibration of damped cracked panels, *International Journal of Fracture* 61 (1993), 123-130.

8. H.D Bui, *Mécanique de la rupture fragile*, Masson, Paris, 1978.

9. J-B Leblond, *Mécanique de la rupture fragile et ductile*, Hermes, Paris, 2003.

10. S. Andrieux, E. Galenne, Harmonic analysis in linear fracture mechanics at moderate frequency contents, *submitted*

11. J.L. Guyader, *Vibration des milieux continus*, Hermes, Paris, 2002.

12. P.A. Raviart, J.M. Thomas, *Introduction à l'analyse numérique des équations aux dérivées partielles*, Masson, Paris, 1983.

13. R. Barsoum, Triangular quarter-point elements as elastic and perfectly-plastic crack tip elements, *International Journal for Numerical Methods in Engineering* 11 (1977), 85-98.

14. H.D. Bui, Associated path-independent J-Integrals for separating mixed modes, *Journal of the Mechanics and Physics of the Solids* 31 (1983), 438-448.

15. M. Attigui, C. Petit, Mixed-Mode Separation in Dynamic Fracture Mechanic : New Path Independent Integral, *Journal of Fracture* 84 (1997), 19-36.

16. P. Destuynder, M. Djaoua, Sur une interprétation de l'intégrale de Rice en théorie de la rupture fragile,

Mathematics Methods in the Applied Sciences 3 (1981), 70-87.

17. P. Destuynder, M. Djaoua, S. Lescure, Quelques remarques sur la mécanique de la rupture élastique, *Journal de Mécanique Théorique et Appliquée* 2 (1983), 113-135.

18. P. Mialon, Calcul de la dérivée d'une grandeur par rapport à un fond de fissure par la méthode théta, *E.D.F. Bulletin de la Direction des Etudes et Recherches - Série C* (1988), 1-28.

19. P. O. Bouchard, F. Bay , Y. Chastel, Numerical modelling of crack propagation: automatic remeshing and comparison of different criteria, *Computer Methods in Applied Mechanics and Engineering* 192 (2003), 3887-3908.

20. *Code_Aster* - Analysis of Structures and Thermomechanics for Surveys and Research. Website: ww.code-aster.org.